

Maps highlight urban-rural differences in achieving Sustainable Development Goals

Yunyu Tian

Wageningen university & Research

N. E. Tsendbazar

Wageningen University and Research Centre, Wageningen, Netherlands

Eveline van Leeuwen

Wageningen University <https://orcid.org/0000-0002-3262-7030>

Martin Herold (✉ martin.herold@wur.nl)

Wageningen University <https://orcid.org/0000-0003-0246-6886>

Article

Keywords:

Posted Date: January 17th, 2022

DOI: <https://doi.org/10.21203/rs.3.rs-1208399/v1>

License: © ⓘ This work is licensed under a Creative Commons Attribution 4.0 International License.

[Read Full License](#)

1 Maps highlight urban-rural differences in achieving 2 Sustainable Development Goals

3 Abstract

4 Land use efficiency, energy efficiency, and air quality are key indicators when assessing urban-
5 related Sustainable Development Goals (SDGs), yet recent trends and trade-offs in and around
6 urban areas worldwide remain largely unknown. We use an Earth Observation approach to map
7 the land-energy-air sustainability nexus and highlight distinct urban-rural gradients worldwide
8 (2000–2015). In the Global South, urban areas perform relatively better in land-energy-air
9 sustainability trends than rural areas, which are the least sustainable in our global comparative
10 analysis. Comparatively, urban areas in the Global North tend to be less sustainable than their
11 surrounding rural regions. Trade-offs among land-energy-air trends are mostly related to
12 energy efficiency versus air quality in urban areas, while trade-offs between land use efficiency
13 and the other two SDGs (energy-air) are more pronounced in rural areas. Integrating satellite-
14 data is crucial for tracking the progress of the land-energy-air nexus and can guide context-
15 specific strategies to account for urban-rural differences in achieving sustainability and creating
16 more liveable environments for improving human wellbeing.

17

18 Introduction

19 The land-energy-air nexus is central to achieving the United Nations (UN) Sustainable
20 Development Goals (SDGs) by 2030 in and around urban areas^{1,2}. With unprecedented
21 urbanization rates, urban dwellers consume up to 60% of global resources²; resource use in
22 surrounding rural areas has also increased rapidly over the recent decade^{3,4}. Simultaneously,
23 between 2010 and 2016, air quality deteriorated for more than half of the world's population,
24 jeopardizing people's health, mainly in cities in Asia and Africa². Such crises of natural resources
25 and environmental quality have become major challenges in achieving SDGs worldwide^{5,6}.
26 Relevant indicators – land use efficiency (SDG 11.3.1), energy efficiency (SDG 7.3.1), and air
27 quality (SDG 11.6.2) – have been established for tracking the sustainable development of cities
28 and communities (SDG 11)¹. The trends of these indicators are connected in several ways (Fig.
29 1), and can only be jointly assessed by using a spatially disaggregated nexus approach; a
30 rapidly expanding new concept for investigating trade-offs and synergies across multiple SDG
31 targets⁷.

32



33

34 **Fig. 1 Conceptual framework of the land-energy-air nexus in the context of**
 35 **urbanization.**

36 Previous research highlights significant urban-rural differences in land use efficiency⁸, energy
 37 consumption⁹, efficiency¹⁰, and air quality¹¹, which vary across regions in the Global North and
 38 South¹². Synergies and trade-offs within the land-energy-air nexus have been mostly studied
 39 for urban ecosystems¹³, i.e. how population growth and built-up land expansion increase energy
 40 consumption and deteriorate air quality in urban areas of South Africa¹⁴. Declining sulfur dioxide
 41 emissions are largely due to a reduced energy intensity in Europe¹⁵, and urban air pollution
 42 could drive down energy intensity in China¹⁶. These studies demonstrate that context-specific
 43 strategies are needed for national SDG target setting^{12,17}, but they remain regional and limited
 44 in scope. In particular, global urban-rural differences in the land-energy-air nexus remain
 45 largely unknown for SDG indicators, such as land use and energy efficiency. We argue that
 46 understanding the local land-energy-air nexus from a global perspective can support context-
 47 specific solutions and win-win-win strategies for multiple SDG targets.

48 Recently, the UN called for a data revolution¹⁸, in particular for the integration of various Earth
 49 Observation (EO) data for the timely monitoring of SDG indicators and nexuses in high spatial
 50 detail⁷. EO-data are open, transparent and have the ability to underpin sustainability analysis in
 51 a consistent way across the world¹⁹. The EO-data allow movement beyond the standard
 52 evaluations of SDG performance that are available as national aggregates and with limited
 53 global comparability^{20,21}. The EO-data are relevant at the level of cities or specific rural-urban
 54 gradients where sustainability actions are expected to make a difference. Recent high-resolution
 55 EO-data can help address the inequality in data availability for the Global South^{12,18}. Integrating
 56 EO-data to explore the land-energy-air nexus will contribute to 'big nexus data'⁷ for guiding
 57 strategies to minimize the trade-offs between SDG targets. Additionally, turning timely EO-data
 58 into direct information for policy-makers is crucial for sustainable developments¹⁸.

59 In this study, we perform an integrated analysis using multiple EO-data (Global Human
60 Settlements, Nighttime Lights, and Near surface PM2.5) to monitor three SDGs: land use
61 efficiency, energy efficiency, and air quality at the 1 km resolution worldwide, from 2000 to
62 2015. Synergy and trade-offs between the three SDG trends are explored using the nexus
63 approach. SDG performances are further scored for comparing urban-rural gradients across
64 continents. By doing so, we unravel the co-occurrences of land-energy-air nexus and provide
65 high spatial detail that international policymakers can use to assess and achieve sustainability.

66

67 Results

68 Global mapping of sustainability trends

69 We reveal that, at the global scale, energy efficiency (SDG 7.3.1) performed better than land
70 use efficiency (SDG 11.3.1) and air quality (SDG 11.6.2) between 2000 and 2015. In nearly
71 60% of the global inhabited grid cells, energy efficiency improved by using less primary energy
72 to produce one unit of economic output (Fig. 2b). In contrast, land use efficiency only increased
73 in 34% of the cells, with less built-up land consumption per capita (Fig. 2a). Improved air
74 quality appeared in about 37% (Fig. 2c), while in nearly 57% of global inhabited grid cells,
75 PM2.5 concentrations exceeded the WHO guideline level of 10 $\mu\text{g}/\text{m}^3$ in 2015 (Supplementary
76 Fig. 1d). These general trends are in line with the global SDG reports²⁰, but our maps present
77 detailed spatial information and allow for regional policy recommendations.

78 With relatively low land use efficiency in 2015 (Supplementary Fig. 1a) and enlarged built-up
79 area per capita since 2000 (Supplementary Fig. 2a), the rural areas of Europe, Northeast US
80 and South Africa need more policy attention to enhance sustainable urbanization (Target 11.3).
81 According to the current status (Supplementary Fig. 1c) and changes of energy intensity (Fig.
82 2b; Supplementary Fig. 2c), the US and rural areas in the Global South need better energy
83 policies to improve their relatively low energy efficiency (Target 7.3). With high PM2.5
84 concentration in 2015 (Supplementary Fig. 1d) and aggravated air pollution since 2000 (Fig. 2c;
85 Supplementary Fig. 2d), Asian countries such as India and China should be targeted for extra
86 efforts to improve air quality (Target 11.6).

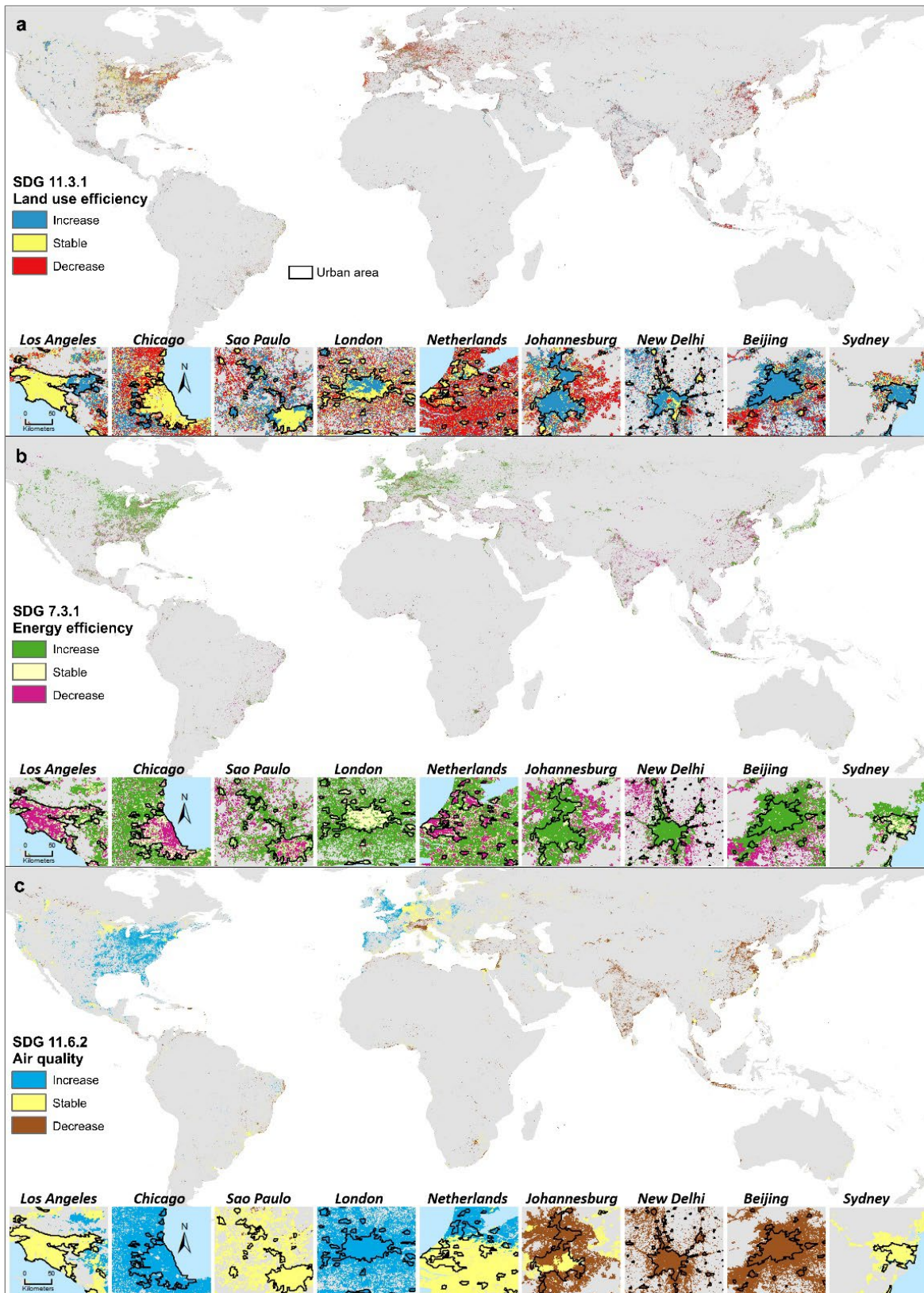
87 Complex patterns in urban-rural gradients

88 Regarding land use efficiency, worldwide, we observe better performance in urban areas
89 compared to rural areas between 2000 and 2015 (Fig. 2a; Supplementary Fig. 2a) as has
90 previously been reported⁸, with the exception of some cities in North America (Supplementary
91 Text 1). Specifically, land use efficiency in most city centers is stable or has increased, while it
92 has decreased in most rural areas. Decreased rural land use efficiency means increased built-up
93 areas occupied by each rural inhabitant; this can be caused by either population decline and/or

94 excessive built-up expansion. In Northwest Europe, the main driver of decreasing land use
95 efficiency can be attributed to the ageing population, which has led to reduced household size²².
96 In Eastern China, decreasing rural land use efficiency is an effect of dispersed industrial land
97 use patterns³, as well as inefficient residential land use caused by rapid built-up construction
98 and rural population decline due to the migration to urban areas^{4,23}. This regional variation
99 shows that the SDG 11.3.1 strategies should depend on local context targeting for population
100 revival or to compact built-up expansion patterns.

101 Regarding energy efficiency, measuring by primary energy consumption/GDP, urban-rural
102 gradient patterns are opposite in the Global North and South (Fig. 2b; Supplementary Fig. 2c).
103 In North US, Canada, and Europe, decreased energy efficiency mostly occurs in metropolitan
104 city centers such as Toronto, Detroit, Los Angeles, Chicago, Paris, and Berlin. Such decreasing
105 urban energy efficiency might be related to a changing sectoral structure and declining
106 economies (Supplementary Text 1). Improved energy efficiency in North US, Europe, and Japan
107 can be mainly attributed to actual decreased energy consumption (Supplementary Fig. 2b). In
108 contrast, energy efficiency in South Asia and Africa increased particularly in urban centers but
109 decreased in their surrounding exurbias (Fig. 2b). Examples include Johannesburg, New Delhi,
110 and Beijing. Improved energy efficiency in China and India mainly results from increased GDP
111 rates, since the energy consumption in most cells increased as well (Supplementary Fig. 2b).
112 Decreased rural energy efficiency in the Global South might be due to the relocation of
113 manufacturing from urban to rural¹¹.

114 Concerning our third SDG, air quality, we did not find a clear urban-rural divide. Instead, our
115 general observation is that air quality is strongly affected by geographical and climate
116 conditions (Fig. 2c). Moderate urban-rural gradients are observed in certain Chinese cities. In
117 2015, air pollution was largely higher in urban centers than in the surrounding suburbs
118 (Supplementary Fig. 1d), but since 2000, increased rates of PM2.5 concentrations in the
119 suburbs have outweighed those in urban centers (e.g. Shenzhen and Chengdu) (Supplementary
120 Fig. 2d). This could be due to environmentally unfriendly factories being moved from urban to
121 rural areas to mitigate urban haze pollution¹¹. Therefore, improving rural air quality is as
122 important as mitigating urban air pollution for the currently most polluted continent: Asia.



123

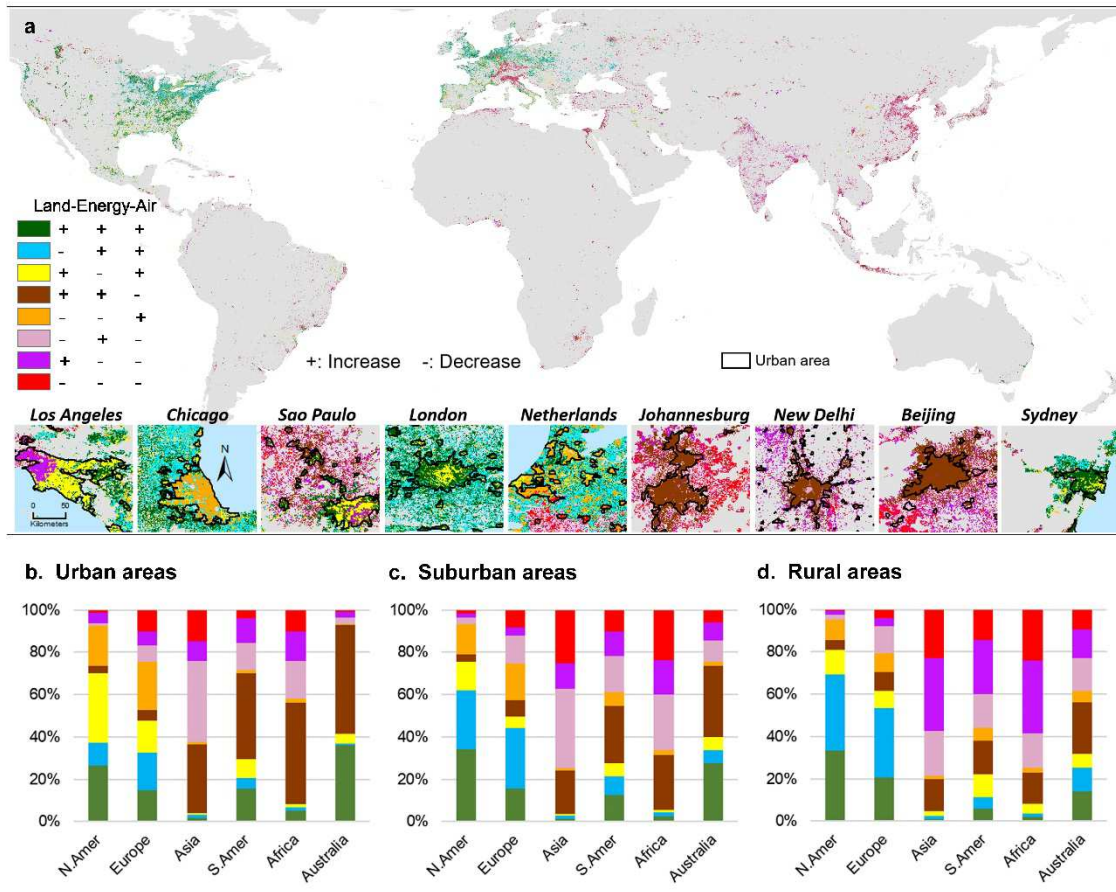
124 **Fig. 2 Global SDG trends between 2000 and 2015 at 1 km resolution. a**, Trend of land
 125 use efficiency, indicated by the change of built-up land per capita. 'Increase' of land use
 126 efficiency means the annual reduction rate of built-up land per capita is over 0.01. **b**, Trend of
 127 energy efficiency, indicated by the change of energy intensity (primary energy consumption per

128 GDP). 'Increase' of energy efficiency means the annual reduction rate of energy intensity is over
129 0.01. **c**, Trend of air quality, indicated by the change of annual mean PM2.5. 'Increase' of air
130 quality means the annual reduction rate of PM2.5 is over 0.01. These grid cells cover all the
131 inhabited areas worldwide. Examples in the figures reflect the urban-rural gradient in typical
132 cities in the Global North and South.

133 Different sustainability trade-offs in urban and rural areas

134 We identified eight synergy/trade-off types for the land-energy-air nexus based on changes of
135 land use efficiency, energy efficiency, and air quality (Fig. 3a), including two fully synergy
136 types: win-win-win type (green areas) and lose-lose-lose type (red areas), as well as six trade-
137 off types. First, we found an urban-rural divide in the land-energy-air nexus. Most identified
138 trade-offs in urban areas concern energy efficiency versus air quality (Fig. 3b), while trade-offs
139 between land use efficiency and the other two SDGs are common in suburban and rural areas
140 (Fig. 3c-d). Secondly, the Global North and South experience opposite directions in trade-offs
141 between resource use (land use and energy) efficiency and air quality. In the Global North, in
142 urban areas, especially in megacities (Fig. 3a-b), energy efficiency declined but air quality
143 improved (orange and yellow areas), while in the Global South, energy efficiency improved, but
144 air quality still declined (chocolate and plum areas).

145 Previous discussions on SDG trade-offs have mostly concerned resource use for social
146 development and adverse environmental impacts; for example, how building infrastructure
147 could negatively impact urban ecosystems¹³ and how using coal to improve energy access
148 would accelerate climate change and air pollution²⁴. Our study adds the spatial aspect of trade-
149 offs between resource use efficiency and air quality. For instance, our maps show that in Asian
150 and African cities, air quality declined even when energy efficiency improved (Fig 3a-b). Since
151 the positive relationship between changes of energy intensity and PM2.5 concentration is
152 demonstrated by this study ($P < 0.01$) and previous research²⁵, governments of countries in Asia
153 and South Africa should not only keep improving primary energy efficiency, but also searching
154 for other effective actions, such as improving the share of renewable energy²⁶ (Supplementary
155 Fig. 3). Such trade-offs inspire local policymakers to rethink if the efforts undertaken are taking
156 effect or just running on a treadmill²⁷.



157

158 **Fig. 3 Land-energy-air nexus between 2000 and 2015.** **a**, Synergy/trade-off types,
 159 classified by the direction of changes in SDG targets. The + and - signs show whether the
 160 performance of SDG target is increased or decreased (+ means target increased as the
 161 indicator decreased). **b-d**, stacked column plots, showing the proportion of synergy/trade-off
 162 types in continents for urban, suburban, and rural areas, respectively.

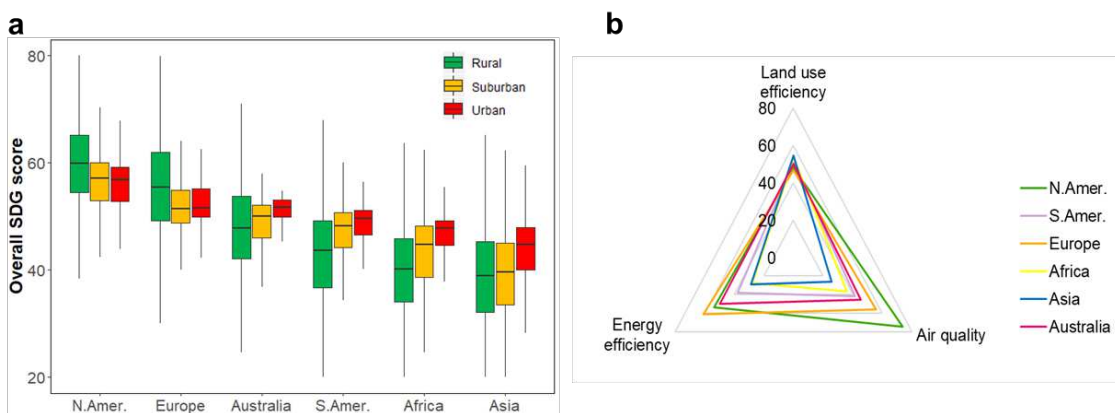
163 **The least sustainable: rural areas in the Global South**

164 The Global South was less sustainable than the Global North during 2000–2015, according to
 165 the overall score of SDG change rates (Fig. 4a; Supplementary Fig. 4). This can be related to
 166 industrialization in developing countries²⁸, as developed countries have increasingly shifted their
 167 focus toward improving environmental quality^{26,27}. Such North-South differences are also
 168 revealed by a previous global study on urban socio-environmental sustainability in terms of
 169 social development, air quality, water, and energy¹². Our analysis highlights even more
 170 dramatic North-South differences in suburban and rural areas compared to the small North-
 171 South difference in urban areas (Fig. 4a; Supplementary Fig. 4). Furthermore, cities that we
 172 identified as more sustainable are also those that people find more livable (Supplementary Fig.
 173 6).

174 In addition to the urban-rural heterogeneity observed for individual SDG trends, the overall
 175 scores of SDG trends show significant urban-suburban-rural differences ($P < 0.05$) (Fig. 4a), and
 176 urban-rural gradients in the Global North and South are opposite. In the Global North, urban
 177 areas are less sustainable than rural areas and have significantly higher rural SDG scores
 178 ($P < 0.05$). In contrast, urban areas are clearly more sustainable than suburban and rural areas
 179 in the South (Fig. 4a), and the lose-lose-lose type (red in Fig. 3b-d) makes up a larger
 180 proportion in rural areas than in urban areas. Thus, improving sustainability particularly in
 181 suburban and rural areas of the Global South is the key to reaching global land-energy-air
 182 targets.

183 With urban sustainability being high on national and international policy agendas^{12,29}, it is
 184 important to note that, currently, urban residents consume more natural resources than rural
 185 residents (Supplementary Fig. 1b). At the same time, our results imply that sustainability issues
 186 in rural areas have become critical for the Global South, with decreased rural resource use
 187 efficiency since 2000 (Fig. 2a-b) and lower rural resource use efficiency compared to urban
 188 areas in 2015 (Supplementary Fig. 1a,c). Since rural areas occupy more land than urban
 189 centres, rural low-resource-use-efficient activities could lead to more unsustainable inhabited
 190 areas overall. Low land use efficiency in newly urbanized areas could replace significant surfaces
 191 of agricultural land and therefore has more adverse environmental impacts than for established
 192 urban land^{3,29}. Furthermore, it is important to revisit the tendency of moving manufacturing
 193 from urban to rural areas, which can improve urban air quality and energy efficiency in the city
 194 of origin but jeopardizes rural sustainability in the longer term¹⁰. With rapid urbanization and
 195 industrialization increasingly occurring in rural regions³, enhancing resource use efficiency is
 196 crucial for turning urbanization into an opportunity for sustainable development in the rural
 197 Global South^{26,30,31}.

198



199

200 **Fig. 4 Urban-suburban-rural gradients and continental difference in SDG scores**
 201 **between 2000 and 2015. a**, Boxplot of overall SDG score, calculated by the average of min-

202 max normalized SDG changes multiplied by 100. Differences between urban, suburban, and
203 rural areas are statistically significant at $P < 0.05$ in each continent, using a t-test. **b**, Radar plot
204 of individual SDG scores, calculated by the min-max normalized SDG changes multiplied by
205 100. Higher score means more sustainable. The median value per continent was taken to
206 reduce the influence of outliers.

207

208 Discussion: better data and approaches for SDG monitoring

209 Our 1 km-gridded maps provide essential spatially detailed information on the land-energy-air
210 nexus for understanding main patterns and trends, and for informing policymakers of effective
211 local and regional actions. First, our data contribute to the SDG data revolution¹⁸. The global
212 maps consistently cover every inhabited cell, which is beneficial for 'data-poor' regions and
213 support their efforts towards the SDGs^{12,18}. Second, previous global reports at national and sub-
214 national levels showed the general trends of SDGs, regardless of local variation within countries,
215 urban/rural areas and even within cities²⁰. Our maps reveal diverse urban and rural issues for
216 the Global North and South, such as deteriorated air quality in the urban South, declined energy
217 efficiency in the urban North and rural South, and decreased land use efficiency in the rural
218 North (Fig. 2–3). National SDG strategies can be more effective when regional and local
219 sustainability challenges are known, i.e. it is important to be aware of differences within
220 megacities or small-sized cities (Fig. 2–3). Third, despite various land-energy-air trade-offs
221 across regions, win-win-win regions exist (see parts of London and Sydney as green areas in
222 Fig. 3a) and should be studied in more detail on why they are able to perform better than
223 others. Local trade-offs reflected by our map (Fig. 3) can guide the context-specific strategies to
224 transform all inhabited areas into win-win-win regions.

225 Potential improvements beyond the current SDG guidelines can be conducted for monitoring
226 SDG indicators at a global scale. For SDG 11.3.1, the official calculation procedures are not
227 easily applicable in population declining regions that exists in various parts of the world³². Our
228 approach was adapted for such circumstances to include the change rate of built-up area per
229 capita, which can indicate land use efficiency in any region. In addition, the rationale of SDG
230 11.3.1 is that cities require orderly urban expansion that makes the land use more efficient, yet
231 the over-densification in urban land is not really considered. For SDG 7.3.1, the official
232 definition of energy intensity is for the supply-side energy of economic activities but the
233 suggested disaggregation methodology is for consumer-side energy³³. In addition, SDGs mainly
234 consider energy efficiency as energy per GDP, yet energy consumption per capita is also
235 important for mitigating the energy crisis³⁴. For SDG 11.6.2, the data sources recommended in
236 the guideline are ground-based observations limited to the regional scale³⁵, regardless of the
237 potential products from remote sensing field, which can provide increasingly fine-scale PM2.5

238 concentration. Including more satellite-based products is important for more disaggregated
239 monitoring of SDGs at a fine scale with large spatial and temporal coverage.

240

241 Methods

242 Improved calculation of land use efficiency

243 SDG 11.3 aims to enhance inclusive and sustainable urbanization and capacity for participatory,
244 integrated, and sustainable human settlement planning and management in all countries by
245 2030²⁰. To achieve this target, cities require an orderly, built-up expansion that makes the land
246 use more efficient. SDG indicator 11.3.1 is officially defined as the ratio of land consumption
247 rate to population growth rate, referred to as land use efficiency (LUE)³². For the measurement,
248 the United Nations Human Settlements Programme (UN-HABITAT) workshop suggests using the
249 built-up area and population within the built-up land³². However, the official definition has a
250 widely-noticed limitation: it is difficult to capture the dynamics of cities with negative or zero
251 population growth^{36,37}. To overcome this limitation, the Joint Research Centre (JRC) has
252 developed the formulation of LUE to built-up area per capita³⁶, and we adopted the calculation
253 of annual change rate from the metadata of SDG 11.3.1:

$$254 \text{ Annual change rate of Built-up area per capita} = \ln \frac{\frac{\text{Built-up area}_{2015}}{\text{Population}_{2015}}}{\frac{\text{Built-up area}_{2000}}{\text{Population}_{2000}}} / 15 \quad (1)$$

255 The improved formulation of LUE expresses a more indicative concept that increased built-up
256 area occupied by each person means decreased land use efficiency³⁶. Negative change rates
257 represent increased land use efficiency, while positive values indicate decreased land use
258 efficiency. Logged change rates can obscure outliers, which are necessary for better
259 visualization of the global gridded map.

260 The Global Human Settlement Layer (GHSL) is the official data source for monitoring SDG
261 11.3.1³². In this study, the GHSL released in 2016 (GHS P2016) was used to calculate built-up
262 area per capita in each 1 km grid cell. The multi-temporal built-up pixels (GHS-BUILT) describe
263 the presence of built-up land at 38 m resolution for a long-term period (1975–2015), which
264 were extracted from Landsat image archives using a Symbolic Machine Learning approach. More
265 detail can be found in Pesaresi and Freire (2016)³⁸. GHS-BUILT has been proven to be accurate
266 and reliable for capturing global built-up changes, even in complex urban centers and low
267 density peri-urban areas^{39,40}. Assuming that built-up area and population are usually consistent
268 in amount, Freire et al. (2015) disaggregated population censuses from Gridded Population of
269 the World (GPW) into 250 m grids according to built-up information in the GHS-BUILT grids⁴¹.
270 This finally resulted in data of population counts per 250 m grid (GHS-POP), disregarding
271 administrative boundaries.

272 Downscaling primary energy

273 National statistics of primary energy consumption in 2000 and 2015 were obtained from the
274 U.S. Energy Information Administration (EIA)⁴². The statistics include coal, petroleum, natural
275 gas, and renewable energy consisting of net nuclear, hydroelectric, and non-hydroelectric
276 renewable electricity. The recommended data source by the UN for SDG 7.3.1³³ is the
277 International Energy Agency (IEA) dataset, which only covers OECD countries⁴³; comparatively,
278 EIA provides free primary energy data for all countries in the world. We compared the primary
279 energy of OECD countries from EIA and IEA, and found that the numbers are similar, which
280 further proves that our data source from EIA is reliable. Although SDG 7.3.1 is for supply-side
281 energy, downscaling consumer-side energy from national statistics to grid cells is feasible
282 according to previous studies^{44,45}.

283 Since energy consumption at the grid level is not available, spatial proxy data can be used to
284 downscale the national statistics^{44,45}. The most common proxy data is population distribution⁴⁵,
285 and recently, the nighttime light dataset has been regarded as a proxy to downscale energy
286 consumption⁴⁴. Previous research often first split the national energy consumption into urban
287 energy and rural energy, and then downscaled this to grid cells separately. However, the
288 national ratio of urban energy consumption is not suitable for all cities because it can cause
289 underestimation for certain mega-cities⁴⁴. Since population and nighttime lights have been
290 widely used to divide urban and rural areas⁴⁶, we combined them as the spatial proxy to
291 downscale national statistical energy consumption. The GHS-POP provides population counts
292 per 250 m grid cell, and a harmonized global nighttime light dataset 1992–2018 provides
293 consistent digital number (DN) values from 0 to 63 at 1 km resolution for the year 2000 and
294 2015⁴⁷. Noise caused by cloud, solar illumination, aurora, and temporal lights have been
295 removed in this nighttime light dataset⁴⁷. We further eliminated night-light emission in non-
296 populated regions to reduce the 'blooming' effect⁴⁸. The remaining bright pixels are relevant to
297 human activities, which can indicate the distribution of energy consumption. As we were aware
298 that most pixels in urban centers have similar highest DN values (63), demographic information
299 (GHS-POP) provide an independent complement to night-light brightness within urban centers.

300 To downscale the national primary energy consumption, we first built linear regression models
301 between energy consumption and two proxy indicators (population and nighttime light) at the
302 country level for the year 2000 and 2015 separately (equation 2). Standardized regression
303 coefficients (β_1 , β_2) in the models were used as weights of two proxy indicators. We adopted a
304 weighted linear downscale approach^{9,49}, since strong linear relationships between energy
305 consumption and population/nighttime lights have been proven in previous studies^{49,50} and this
306 study (Supplementary Fig. 7). Based on equation (3), we generated primary energy
307 consumption maps at the 1 km grid level for 2000 and 2015.

308 $Energy_{country} = \beta_1 Light_{country} + \beta_2 Population_{country}$ (2)

309 $Energy_{grid-i} = Energy_{country} \times \left(\beta_1 \times \frac{Light_{grid-i}}{Light_{country}} + \beta_2 \times \frac{Population_{grid-i}}{Population_{country}} \right)$ (3)

310 Our estimates of gridded energy consumption were validated by the statistical energy
 311 consumption regionally, both at the state level in the United States⁵¹ and at the neighborhood
 312 level in the Netherlands⁵² for the year 2015. The validation results show that our estimated
 313 gridded maps are generally reliable and in line with statistical data at the state/neighborhood
 314 level (Supplementary Fig. 8a–b). We also compared our gridded map with the existing global
 315 gridded anthropogenic heat flux dataset in 2015⁴⁵ and observed deviations from the one-to-one
 316 line (Supplementary Fig. 8c). Such deviations are possibly caused by different statistical data
 317 sources and methods that the existing dataset⁴⁵ only used population as spatial proxy while we
 318 added nighttime light data to reduce the uncertainty of downscaling.

319 Energy efficiency

320 SDG 7.3 aims to double the global rate of improvement in energy efficiency by 2030, which
 321 requires tracking of SDG indicator 7.3.1: energy intensity across the world. Energy intensity is
 322 measured as the primary energy per GDP. A global gridded GDP dataset is available for the year
 323 2000 and 2015, based on sub-national and national GDP per capita, and gridded population
 324 (GHS-POP)⁵³. We used the obtained gridded energy consumption and gridded GDP to calculate
 325 the trend of SDG 7.3.1 between 2000 and 2015:

326 $Annual\ change\ rate\ of\ Energy\ intensity = \ln \frac{\frac{Energy\ consumption_{2015}}{GDP_{2015}}}{\frac{Energy\ consumption_{2000}}{GDP_{2000}}} / 15$ (4)

327 Negative change rates indicate improved energy efficiency (less energy is used to produce one
 328 unit of economic output), while positive numbers indicate decreased energy efficiency.

329 Air quality represented by PM2.5

330 The Global Annual PM2.5 Grids provide annual concentrations (micrograms per cubic meter) of
 331 ground-level fine particulate matter (PM2.5) at 1 km resolution from 1998 to 2016⁵⁴. The PM2.5
 332 concentration was estimated by aerosol optical depth from multiple satellite products (MISR,
 333 MODIS Dark Target, MODIS and SeaWiFS Deep Blue, and MODIS MAIAC), with dust and sea-
 334 salt removed. Global ground-based measurements were used to predict and adjust for the
 335 residual PM2.5 bias per grid cell in the initial satellite-derived values by Geographically
 336 Weighted Regression (GWR). The resultant PM2.5 estimates were highly consistent ($R^2 = 0.81$)
 337 with out-of-sample cross-validated ground-based measurements⁵⁴. With the relatively high
 338 accuracy for inhabited land, this product is widely used to analyze temporal dynamics of air
 339 quality in small to large cities internationally⁵⁵. To monitor SDG 11.6.2 – annual mean levels of

340 fine particulate matter (e.g. PM2.5 and PM10) in cities – we used this product to produce the
341 global 1 km map of SDG 11.6.2 trend:

$$342 \text{ Annual change rate of PM2.5} = \ln \frac{PM2.5 \text{ concentration}_{2015}}{PM2.5 \text{ concentration}_{2000}} / 15 \quad (5)$$

343 Negative change rates indicate improved air quality (less PM2.5 concentration), while positive
344 numbers represent declined air quality.

345 Mapping land-energy-air nexus

346 Nexus approaches are highly recommended for analysis of trade-offs among SDG
347 indicators^{5,7,56}. Statistical models and diverse indicators were used for quantitative nexus
348 analysis; indicators that can combine nexus variables into a single number are common in
349 nexus research. Mapping out the score to qualify interactions between SDG targets is suggested
350 as a simple way to rate local trade-offs for practical policy making²⁴. Based on this theory, we
351 combined the directions of multiple SDG trends into archetypes of land-energy-air nexus for
352 each 1 km grid cell. Two fully synergy types with consistent change directions of land-energy-
353 air targets, and six trade-off types with inconsistent change directions among land-energy-air
354 nexus were detected in this study.

355 Scoring the performance of land-energy-air SDGs

356 Min-max normalized scores are typically used for comparing performance of SDG targets and
357 indicators across regions⁶. Here, we also produced individual SDG scores based on the change
358 rate of each SDG indicator (equation 6), ranging from 0 to 100. Although the change rate was
359 logged, many outliers with extreme values still remain in the obtained change rate map, which
360 can influence the min-max normalization. Thus, we removed statistical outliers for each change
361 rate map before the min-max normalization. Normalized change rates needed to be inverted to
362 get the final SDG score because increasing SDG indicator signifies decreasing SDG target. In
363 doing so, higher scores represent better performance towards the SDG target (e.g. energy
364 efficiency) as the corresponding SDG indicator (e.g. energy intensity) decreases. The overall
365 SDG score was calculated by the average of three individual SDG scores, representing the
366 overall performance of land-energy-air nexus. Finally, we revealed the continental differences in
367 individual SDG performance and urban-suburban-rural gradient in overall SDG performance
368 (Fig. 4).

$$369 \text{ SDG score}_{grid-i} = \left(1 - \frac{\text{Change rate}_{grid-i} - \text{minimum global change rate}}{\text{maximum global change rate} - \text{minimum global change rate}}\right) \times 100 \quad (6)$$

370 Uncertainties and limitations

371 Although the GHSL dataset is the best option for monitoring land use efficiency, there are
372 several limitations in GHS-BUILT and GHS-POP. For GHS-BUILT, the identification of built-up

373 land in rural areas is less accurate than that in urban areas^{39,40}. Built-up land in rural areas is
374 scattered and rare, making the previous global land cover products (e.g. CCI-LC and MOD500)
375 almost entirely neglected small settlements within cropland³⁹. Until 2016, the GHSL captured
376 built-up land (manmade roofs) in rural areas at 38 m resolution with temporal consistent
377 (1975–1990–2000–2015), but there still exist potential risks of overestimating settlement areas
378 due to 30 m Landsat images⁵⁷, such as for the rural Tuscany region³⁹. GUF has higher resolution
379 than GHSL for built-up land, but its usefulness is limited by inadequate temporal coverage^{58,59}.
380 Multi-temporal and refined global maps for the built-up land are needed for improving the
381 accuracy of monitoring land use efficiency in rural areas. Moreover, the GHS-POP was mainly
382 disaggregated from census data and distributed proportionally over build-up density. Yet,
383 functional land use of buildings and their height were not considered in the process of
384 population disaggregation⁶⁰. By including this information on buildings across the world, more
385 feasible gridded population and land use efficiency can be produced.

386 Our country-level energy data reflects the consumer-side, which makes it possible to
387 disaggregate by nighttime lights and population. However, the SDG indicator 7.3.1 suggested
388 by the UN, reflects the supply-side energy. For rural areas in Asia, consumer-side energy might
389 be lower than supply-side energy, since a portion of secondary energy consumed by urban
390 residents is produced in rural areas using the primary energy (e.g. the coal used by power
391 stations to generate electricity)⁴⁴. Although we combined two spatial proxy indicators –
392 nighttime lights and population – some uncertainties still exist in the disaggregation process
393 from top to bottom. For instance, the distribution of energy consumption within urban centers
394 has been based mainly on the gridded population because the nighttime lights in urban grid
395 cells tend to be equal to the maximum digital number (63). This implies that each urban
396 resident consumes the same amount of energy in any given city. Given the uncertainties at the
397 local scale, reporting supply-side energy data from the bottom, such as collecting from factories
398 would be necessary to reduce the dependency on country-level statistics and to further improve
399 the guideline for SDG 7.3.1.

400 The nexus concept is still evolving and it is challenging to univocally adopt a default approach
401 and standardize indicators⁵⁶, particularly for the quantification at a global scale. Most previous
402 research explored the general trade-offs between SDG targets across regions, and the global
403 trade-offs on land-energy-air mainly remains at the theoretical level^{13,61}. We provided a new
404 perspective on mapping trade-offs and synergies among SDG indicators globally. Various local
405 trade-offs and synergies we detected could provide accurate information for policy makers.
406 Since we were limited by the temporal coverage of public global data, we only explored
407 interactions based on the directions of SDG trends between two epochs. Future mapping studies
408 can use long-time-series datasets with multiple epochs to score the interactions between SDG
409 indicators for each grid cell²⁴.

411 Reference

- 412 1. United Nations. Global indicator framework for the Sustainable Development Goals and
 413 targets of the 2030 Agenda for Sustainable Development. *Work Stat. Comm. Pertain. to*
 414 *2030 Agenda Sustain. Dev.* (2020).
- 415 2. United Nations. The sustainable development goals report 2019. *United Nations Publ.*
 416 *issued by Dep. Econ. Soc. Aff.* 64 (2019).
- 417 3. Jiang, G., Ma, W., Dingyang, Z., Qinglei, Z. & Ruijuan, Z. Agglomeration or dispersion?
 418 Industrial land-use pattern and its impacts in rural areas from China's township and
 419 village enterprises perspective. *J. Clean. Prod.* (2017). doi:10.1016/j.jclepro.2017.04.152
- 420 4. Wang, H., Wang, L., Su, F. & Tao, R. Rural residential properties in China: Land use
 421 patterns, efficiency and prospects for reform. *Habitat Int.* (2012).
 422 doi:10.1016/j.habitatint.2011.06.004
- 423 5. Bleischwitz, R. *et al.* Resource nexus perspectives towards the United Nations Sustainable
 424 Development Goals. *Nat. Sustain.* **1**, 737–743 (2018).
- 425 6. Zeng, Y. *et al.* Environmental destruction not avoided with the Sustainable Development
 426 Goals. *Nat. Sustain.* **3**, 795–798 (2020).
- 427 7. Liu, J. *et al.* Nexus approaches to global sustainable development. *Nat. Sustain.* **1**, 466–
 428 476 (2018).
- 429 8. Schiavina, M. *et al.* Multi-scale estimation of land use efficiency (SDG 11.3.1) across 25
 430 Years Using Global Open and Free Data. *Sustain.* **11**, 1–25 (2019).
- 431 9. van Vuuren, D. P., Lucas, P. L. & Hilderink, H. Downscaling drivers of global
 432 environmental change: Enabling use of global SRES scenarios at the national and grid
 433 levels. *Glob. Environ. Chang.* **17**, 114–130 (2007).
- 434 10. Tan, L. M., Arbabi, H., Densley Tingley, D., Brockway, P. E. & Mayfield, M. Mapping
 435 resource effectiveness across urban systems. *npj Urban Sustain.* **1**, 1–14 (2021).
- 436 11. Han, L., Zhou, W. & Li, W. Increasing impact of urban fine particles (PM_{2.5}) on areas
 437 surrounding Chinese cities. *Sci. Rep.* (2015). doi:10.1038/srep12467
- 438 12. Nagendra, H., Bai, X., Brondizio, E. S. & Lwasa, S. The urban south and the predicament
 439 of global sustainability. *Nat. Sustain.* **1**, 341–349 (2018).
- 440 13. Maes, M. J. A., Jones, K. E., Toledano, M. B. & Milligan, B. Mapping synergies and trade-
 441 offs between urban ecosystems and the sustainable development goals. *Environ. Sci.*

- 442 *Policy* **93**, 181–188 (2019).
- 443 14. Shikwambana, L. & Tsoeleng, L. T. Impacts of population growth and land use on air
444 quality. A case study of Tshwane, Rustenburg and Emalahleni, South Africa. *South African*
445 *Geogr. J.* (2020). doi:10.1080/03736245.2019.1670234
- 446 15. Rafaj, P., Amann, M., Siri, J. & Wuester, H. Changes in European greenhouse gas and air
447 pollutant emissions 1960–2010: Decomposition of determining factors. *Clim. Change*
448 (2014). doi:10.1007/s10584-013-0826-0
- 449 16. Hou, J., Wang, J., Chen, J. & He, F. Does urban haze pollution inversely drive down the
450 energy intensity? A perspective from environmental regulation. *Sustain. Dev.* **28**, 343–
451 351 (2020).
- 452 17. Blanchard, J. L. *et al.* Linked sustainability challenges and trade-offs among fisheries,
453 aquaculture and agriculture. *Nat. Ecol. Evol.* (2017). doi:10.1038/s41559-017-0258-8
- 454 18. United Nations. A World that Counts: Mobilising the Data Revolution for Sustainable
455 Development. *IEAG* (2020). doi:10.7551/mitpress/12439.003.0018
- 456 19. Cochran, F., Daniel, J., Jackson, L. & Neale, A. Earth observation-based ecosystem
457 services indicators for national and subnational reporting of the sustainable development
458 goals. *Remote Sens. Environ.* **244**, 111796 (2020).
- 459 20. Council, S. & Council, S. *SDG Progress Report 2020. United Nations* (2020).
- 460 21. The World Bank and International Energy Agency. Global Tracking Framework 2017. in
461 *Global Tracking Framework: Progress toward Sustainable energy* (2017).
- 462 22. Franklin, R. S. & van Leeuwen, E. S. For Whom the Bells Toll: Alonso and a Regional
463 Science of Decline. *Int. Reg. Sci. Rev.* **41**, 134–151 (2018).
- 464 23. Yu, X. J. & Ng, C. N. Spatial and temporal dynamics of urban sprawl along two urban-
465 rural transects: A case study of Guangzhou, China. *Landsc. Urban Plan.* **79**, 96–109
466 (2007).
- 467 24. Nilsson, M., Griggs, D. & Visbeck, M. Policy: Map the interactions between Sustainable
468 Development Goals. *Nature* **534**, 320–322 (2016).
- 469 25. Chen, J., Zhou, C., Wang, S. & Li, S. Impacts of energy consumption structure, energy
470 intensity, economic growth, urbanization on PM_{2.5} concentrations in countries globally.
471 *Appl. Energy* **230**, 94–105 (2018).
- 472 26. Akram, R., Chen, F., Khalid, F., Ye, Z. & Majeed, M. T. Heterogeneous effects of energy
473 efficiency and renewable energy on carbon emissions: Evidence from developing

- 474 countries. *J. Clean. Prod.* (2020). doi:10.1016/j.jclepro.2019.119122
- 475 27. Reflections on Sustainability. *Nat. Sustain.* **4**, 921 (2021).
- 476 28. Sadorsky, P. Do urbanization and industrialization affect energy intensity in developing
477 countries? *Energy Econ.* (2013). doi:10.1016/j.eneco.2013.01.009
- 478 29. Zhou, W. *et al.* Beyond city expansion: multi-scale environmental impacts of urban
479 megaregion formation in China. *Natl. Sci. Rev.* (2021). doi:10.1093/nsr/nwab107
- 480 30. Zhou, W., Pickett, S. & McPhearson, T. Conceptual Frameworks Facilitate Integration for
481 Transdisciplinary Urban Science. *npj Urban Sustain.* 1–11 doi:10.1038/s42949-020-
482 00011-9
- 483 31. Liu, Y. Exploring the relationship between urbanization and energy consumption in China
484 using ARDL (autoregressive distributed lag) and FDM (factor decomposition model).
485 *Energy* **34**, 1846–1854 (2009).
- 486 32. UN-Habitat. Metadata on SDGs Indicator 11.3.1. 1–12 (2018).
- 487 33. United Nations. Metadata on SDGs Indicator 7.3.1. (2021). Available at:
488 <https://unstats.un.org/sdgs/metadata/files/Metadata-07-03-01.pdf>.
- 489 34. Sikder, S. K., Nagarajan, M., Kar, S. & Koetter, T. A geospatial approach of downscaling
490 urban energy consumption density in mega-city Dhaka, Bangladesh. *Urban Clim.* **26**, 10–
491 30 (2018).
- 492 35. United Nations. Metadata on SDGs Indicator 11.6.2. (2021). Available at:
493 <https://unstats.un.org/sdgs/metadata/files/Metadata-11-06-02.pdf>.
- 494 36. Paresi, M., Melchiorri, M., Siragusa, A. & Kemper, T. *Atlas of the Human Planet. Mapping
495 Human Presence on Earth with the Global Human Settlement Layer.* (2017).
496 doi:10.2788/889483
- 497 37. Melchiorri, M., Pesaresi, M., Florczyk, A., Corbane, C. & Kemper, T. Principles and
498 Applications of the Global Human Settlement Layer as Baseline for the Land Use
499 Efficiency Indicator—SDG 11.3.1. *ISPRS Int. J. Geo-Information* **8**, 96 (2019).
- 500 38. Pesaresi, M. & Freire, S. GHS-SMOD R2016A - GHS settlement grid, following the REGIO
501 model 2014 in application to GHSL Landsat and CIESIN GPW v4-multitemporal (1975-
502 1990-2000-2015). *Eur. Comm. Jt. Res. Cent.* (2016).
- 503 39. Klotz, M., Kemper, T., Geiß, C., Esch, T. & Taubenböck, H. How good is the map? A multi-
504 scale cross-comparison framework for global settlement layers: Evidence from Central
505 Europe. *Remote Sens. Environ.* (2016). doi:10.1016/j.rse.2016.03.001

- 506 40. Leyk, S., Uhl, J. H., Balk, D. & Jones, B. Assessing the accuracy of multi-temporal built-
507 up land layers across rural-urban trajectories in the United States. *Remote Sens. Environ.*
508 (2018). doi:10.1016/j.rse.2017.08.035
- 509 41. Freire, S., Kemper, T., Pesaresi, M., Florczyk, A. & Syrris, V. Combining GHSL and GPW
510 to improve global population mapping. in *International Geoscience and Remote Sensing*
511 *Symposium (IGARSS)* (2015). doi:10.1109/IGARSS.2015.7326329
- 512 42. U.S. Energy Information Administration (EIA). International Energy Statistics: Total
513 Primary Energy Consumption. Available at:
514 <https://www.eia.gov/international/data/world/total-energy/>.
- 515 43. IEA. *World Energy Statistics and Balances. IEA World Energy Statistics and Balances*
516 *(database)* (2018).
- 517 44. Yang, W. *et al.* Data Descriptor: A new global anthropogenic heat estimation based on
518 high-resolution nighttime light data. *Sci. Data* **4**, 1–11 (2017).
- 519 45. Jin, K. *et al.* A new global gridded anthropogenic heat flux dataset with high spatial
520 resolution and long-term time series. *Sci. Data* **6**, 1–14 (2019).
- 521 46. Zhou, Y. *et al.* A global map of urban extent from nightlights. *Environ. Res. Lett.* **10**,
522 2000–2010 (2015).
- 523 47. Li, X., Zhou, Y., Zhao, M. & Zhao, X. A harmonized global nighttime light dataset 1992–
524 2018. *Sci. Data* **7**, 1–9 (2020).
- 525 48. Wang, L. *et al.* Mapping population density in China between 1990 and 2010 using
526 remote sensing. *Remote Sens. Environ.* **210**, 269–281 (2018).
- 527 49. Dong, Y., Varquez, A. C. G. & Kanda, M. Global anthropogenic heat flux database with
528 high spatial resolution. *Atmos. Environ.* **150**, 276–294 (2017).
- 529 50. Xiao, H. *et al.* Spatio-temporal simulation of energy consumption in China’s provinces
530 based on satellite night-time light data. *Appl. Energy* **231**, 1070–1078 (2018).
- 531 51. U.S. Energy Information Administration (EIA). State Energy Data System. (2021).
532 Available at: <https://www.eia.gov/state/seds/seds-data-complete.php?sid=US>.
- 533 52. Netherlands, S. Wijk- en Buurtkaart 2017. (2018).
- 534 53. Kummu, M., Taka, M. & Guillaume, J. H. A. Gridded global datasets for Gross Domestic
535 Product and Human Development Index over 1990-2015. *Sci. Data* **5**, 1–15 (2018).
- 536 54. Van Donkelaar, A. *et al.* Global Estimates of Fine Particulate Matter using a Combined
537 Geophysical-Statistical Method with Information from Satellites, Models, and Monitors.

- 538 *Environ. Sci. Technol.* **50**, 3762–3772 (2016).
- 539 55. Liang, L. & Gong, P. Urban and air pollution: a multi-city study of long-term effects of
540 urban landscape patterns on air quality trends. *Sci. Rep.* (2020). doi:10.1038/s41598-
541 020-74524-9
- 542 56. Næss, J. S., Cavalett, O. & Cherubini, F. The land–energy–water nexus of global
543 bioenergy potentials from abandoned cropland. *Nat. Sustain.* **4**, 525–536 (2021).
- 544 57. Sabo, F. *et al.* Comparison of built-up area maps produced within the global human
545 settlement framework. *Trans. GIS* **22**, 1406–1436 (2018).
- 546 58. Esch, T. *et al.* Breaking new ground in mapping human settlements from space – The
547 Global Urban Footprint. *ISPRS J. Photogramm. Remote Sens.* (2017).
548 doi:10.1016/j.isprsjprs.2017.10.012
- 549 59. Liu, C. *et al.* Automatic extraction of built-up area from ZY3 multi-view satellite imagery:
550 Analysis of 45 global cities. *Remote Sens. Environ.* (2019).
551 doi:10.1016/j.rse.2019.03.033
- 552 60. Freire, S., Macmanus, K., Pesaresi, M. & Doxsey-Whitfield, E. Development of new open
553 and free multi-temporal global population grids at 250 m resolution Validation of remote
554 sensing derived emergency mapping maps View project Megacities View project. (2016).
- 555 61. Fuso Nerini, F. *et al.* Mapping synergies and trade-offs between energy and the
556 Sustainable Development Goals. *Nat. Energy* **3**, 10–15 (2018).
- 557

Supplementary Files

This is a list of supplementary files associated with this preprint. Click to download.

- [4.Supplementary.docx](#)